



Scan code to view VIDEO

THREE-DIMENSIONAL QUANTIFICATION OF INTRARETINAL CYSTOID SPACES ASSOCIATED WITH FULL-THICKNESS MACULAR HOLE

KOTARO TSUBOI, MD,*† YUKUN GUO, MS,‡ JIE WANG, MS,*‡ ELIZABETH WHITE, MS,* SAM MERSHON, MS,* MOTOHIRO KAMEI, MD,† DAVID HUANG, MD,*‡ YALI JIA, PhD,*‡ THOMAS S. HWANG, MD,* STEVEN T. BAILEY, MD*

Purpose: To evaluate intraretinal cystoid spaces in patients with idiopathic macular hole (MH).

Methods: Retrospective cohort study included consecutive patients with full-thickness MH who underwent successful MH surgery and 12 months of follow-up. Custom software was applied to preoperative optical coherence tomography scans to generate fluid volume. Inner fluid volume was defined as cystoid spaces in the inner nuclear layer, and outer fluid volume was defined as cystoid spaces in Henle fiber layer of the outer nuclear layer.

Results: Thirty-nine eyes from 39 participants were included. Postoperative 12-month visual acuity correlated with both inner fluid volume and minimum MH size (both $P < 0.05$) but not outer fluid volume. Inner fluid volume positively correlated with minimum MH size ($P = 0.0003$). After accounting for minimum MH size with multivariable analysis, inner fluid volume effect on VA remained significant ($P = 0.025$). After dividing inner fluid volume into tertiles, mean baseline visual acuity was 20/50 in eyes with small inner fluid volume, and was 20/125 in eyes with large inner fluid volume ($P = 0.0039$). Mean postoperative 12-month visual acuity was 20/20 in eyes with small inner fluid volume compared with 20/32 in eyes with large inner fluid volume ($P = 0.019$).

Conclusion: Increased inner fluid volume was associated with worse postoperative VA.

RETINA 42:2267–2275, 2022

Intraretinal cystoid spaces in patients with macular hole (MH) are commonly observed on optical coherence tomography (OCT) adjacent to the hole.^{1–6} They are located in the inner nuclear layer (INL) and in the Henle fiber layer (HFL) of the outer nuclear layer (ONL). Size and shape of intraretinal cystoid spaces are different depending on the location in the retina.^{3,5} The intraretinal cystoid spaces can occur in the early stage of MH, Stage 1-B by Gass classification,⁷ and intraretinal cystoid space are observed to increase in later stages.⁶ On fluorescein angiography, the absence of dye leakage has led to the hypothesis that the intraretinal cystoid spaces in MH originate from the tractional macular abnormalities.⁵

Prior studies evaluated intraretinal cystoid spaces two dimensionally, such as OCT B-scan and *en-face* OCT.^{3,5,6} Studies with *en-face* OCT demonstrated that the inner cystoid spaces in MH are presumably associated with Z-shaped Müller cells,^{3,5} which has been

observed in the perifoveal region on histological studies.^{3,8} The characteristic Z-shaped Müller cells course from the external limiting membrane to the inner limiting membrane toward the periphery. The oblique portion of this course corresponds to the ONL and the HFL. The intraretinal cystoid spaces configuration on *en-face* OCT resembles the “spoke-wheel” pattern that correlates with the anatomical configuration of the radially oriented Z-shaped Müller cells.^{3,5} Although these studies demonstrated the characteristics of the intraretinal cystoid spaces in MH,^{3,5,6} there has been no study quantifying the intraretinal cystoid spaces three dimensionally.

Emerging OCT technology can extract and quantify the three-dimensional retinal cystoid spaces as volume from high-resolution structural OCT.^{9–11} In this study, novel OCT volume rendering software was used to study the distribution and quantity of intraretinal cystoid spaces in eyes with different stages of idiopathic

MH. Because cystoid macular edema can be associated with retinal degeneration, we hypothesized that increased intraretinal cystoid space in MH may be associated with worse postoperative visual acuity.

Methods

This retrospective study adhered to the tenets of the Declaration of Helsinki was approved by the Institutional Review Boards of the Aichi Medical University and the Oregon Health and Science University. Consecutive patients diagnosed with MH who had undergone successful primary MH surgery at the Department of Ophthalmology, Aichi Medical University Hospital, from October 1, 2016, to June 30, 2019. Data analysis with custom OCT software began in December of 2020. All study participants were required to be pseudophakic for their one-year postoperative visit. Patients with poor-quality images (signal strength index < 50), axial length greater than 26.5 mm, chronic MH with longer than 12-month disease duration at presentation, and the presence of other retinal diseases, such as epiretinal membrane, myopic foveoschisis, and retinal vascular diseases, were excluded. Study participants with diabetes were

excluded. Only one eye of each study participant was included in this study.

Twenty-five-gauge or twenty-seven-gauge vitrectomy was performed with the patient under local anesthesia using a variety of surgical vitrectomy systems (Constellation Vision System; Alcon Laboratories, Inc, Fort Worth, TX; or EVA Phaco-Vitrectomy System; DORC, Zuidland, the Netherlands). Phacemulsification and intraocular lens implantation were performed in all phakic eyes. Inner limiting membrane peeling was performed within a 3-mm center on the fovea using Brilliant Blue G (inner limiting membrane blue; DORC) in all eyes. Fluid–air exchange was performed, and if needed, a long-acting gas, such as 20% sulfur hexafluoride or 6% perfluoro propane, was applied to the vitreous cavity. All patients were required a prone position until MH closure was confirmed by OCT, which was performed in gas-filled eyes.

All study participants underwent a comprehensive ocular examination, including measurement of the best-corrected visual acuity with Landolt C chart and axial length measurement using AL scan (Nidek, Gamagori, Japan). Optical coherence tomography was performed using a spectral-domain OCT (RTVue XR Avanti, Optovue, Inc, Fremont, CA) before MH surgery. A small subgroup of study participants had more than one OCT scan on different days before the surgery.

Volume rendered OCT was generated from 3×3 -mm macular scans using the RTVue-XR Avanti (Optovue, Inc, Fremont, CA) centered on the fovea. Scans were exported for custom processing using MATLAB (MathWorks)-based software. Guided bidirectional graph search method was used to segment retinal tissue boundaries of the intraretinal cystoid spaces in the INL and in the HFL of the ONL (Figure 1).¹² All 304 B-scan images were merged to generate volume-rendered OCT. We defined inner fluid volume as cystoid spaces in the INL and outer fluid volume as cystoid spaces in the HFL of the ONL. Fluid volume was calculated as the product of the number of detected voxels and the voxel dimension ($10 \times 10 \times 3.0 \mu\text{m}^3$) in each scan. We evaluated inner fluid volume, outer fluid volume, and total fluid volume that is the sum of inner fluid volume and outer fluid volume.

Minimum MH size was defined as the shortest horizontal line of the hole, and basal MH size was defined as horizontal line of the hole just above retinal pigmental epithelium. The International Vitreomacular Traction Study Group classification¹³ was used to define MH size based on OCT images as follows: small MH is minimum MH size of $\leq 250 \mu\text{m}$, medium MH is minimum MH size of $>250 \mu\text{m}$ but $\leq 400 \mu\text{m}$,

From the *Casey Eye Institute, Oregon Health & Science University, Portland, Oregon; †Department of Ophthalmology, Aichi Medical University, Nagakute, Japan; and ‡Department of Biomedical Engineering, Oregon Health & Science University, Portland, Oregon 97239.

Supported by the National Institutes of Health (R01EY027833, R01EY024544, P30EY010572); William and Mary Greve Special Scholar Award, and unrestricted departmental funding from the Research to Prevent Blindness (New York, NY). The funding source had no role in the design and conduct of the study; collection, management, analysis, and interpretation of the data; preparation, review, or approval of the manuscript; and decision to submit the manuscript for publication.

Presented at ARVO2021 in virtual meeting at May 1 2021.

None of the authors has any financial/conflicting interests to disclose.

Supplemental digital content is available for this article. Direct URL citations appear in the printed text and are provided in the HTML and PDF versions of this article on the journal's Web site (www.retinajournal.com).

Oregon Health & Science University (OHSU) and Drs. Jia, Huang, and Bailey have a significant financial interest in Optovue Inc, a company that may have a commercial interest in the results of this research and technology. These potential conflicts of interest have been reviewed and managed by the OHSU. Dr Tsuboi reported receiving personal fees from Bayer, Novartis Pharma, Santen, and Alcon Japan outside the submitted work. Dr. Kamei has a financial interest (to institution) in HOYA Surgical Optics, Abbott Medical Optics, Novartis Pharma KK, Pfizer Japan, Inc., HAN-DAYA Co., Ltd., TOMEY Co., Ltd., Kowa Co., Ltd., Santen Co., Ltd., Senju Co., Ltd., Otsuka Co., Ltd., and Alcon Japan Ltd. outside the submitted work. No other disclosures were reported.

Reprint requests: Steven T. Bailey, MD, Casey Eye Institute, Oregon Health & Science University, 515 SW Campus Dr., Portland, OR 97239; e-mail: bailstev@ohsu.edu

Table 1. Patient Characteristics of the Study Participants

| Parameter | Data Value (N = 39) |
|--|---|
| Age, mean (SD) [range], y | 65 (8) [45–79] |
| Sex, no. (%) | |
| Men | 15 (38) |
| Women | 24 (62) |
| Baseline BCVA, mean (SD) [range], logMAR | 0.63 (0.30) [0.15–1.3] |
| 1-year BCVA, mean (SD) [range], logMAR | 0.12 (0.16) [-0.079–0.52] |
| Axial length, mean (SD) [range], mm | 24.0 (1.1) [21.9–26.0] |
| Phakia before surgery, no. (%) | 36 (92) |
| Lens opacification, no. (%) | |
| Grade 2 | 11 (28%) |
| Grade 3 | 28 (72%) |
| Gas tamponade, no. (%) | |
| Air | 3 (8) |
| 20% SF ₆ | 9 (23) |
| 6% C ₃ F ₈ | 27 (69) |
| MH size based on International Vitreomacular Traction Study classification | |
| Small, no. (%) | 10 (26%) |
| Medium, no. (%) | 11 (28%) |
| Large, no. (%) | 18 (46%) |
| Presence of VMT, no. (%) | 16 (41%) |
| Minimum MH size, mean (SD) [range], μm | 379 (161) [80–735] |
| Basal MH size, mean (SD) [range], μm | 810 (243) [288–1,222] |
| Inner fluid volume, mean (SD) [range], mm ³ | 0.015 (0.014) [0.00–0.060] |
| Outer fluid volume, mean (SD) [range], mm ³ | 0.10 (0.074) [0.79 \times 10 ⁻⁵ to 0.28] |
| Total fluid volume, mean (SD) [range], mm ³ | 0.12 (0.079) [0.79 \times 10 ⁻⁵ to 0.28] |

BCVA, best-corrected visual acuity.

direct connections were observed between the inner fluid and the outer fluid.

Quantification of Fluid Volume and Macular Hole Size

Quantitative analysis demonstrated that the mean (SD) inner fluid volume was 0.015 (0.014) mm³, and the mean (SD) outer fluid volume was 0.10 (0.074) mm³. The inner fluid volume was significantly smaller than the outer fluid volume ($P < 0.0001$, Wilcoxon-signed rank test). To evaluate the fluid distribution pattern between inner and outer fluid volume, we calculated the percentage of the fluid volume within and outside a 1.5-mm circle centered on the fovea. The majority of the outer fluid volume (mean [SD] percentage, 87.5 [13.1%]) was within the 1.5-mm circle. By contrast, only 43.6 (29.0) % of the inner fluid volume was present within the 1.5-mm circle ($P < 0.0001$ by Paired *t*-test).

The inner fluid volume significantly correlated with the minimum MH size ($R = 0.54$, [95% CI, 0.28–0.73], $P = 0.0003$), in contrast to the outer fluid volume ($R = 0.064$, [95% CI, -0.26 to 0.37], $P = 0.70$) and the total fluid volume ($R = 0.16$, [95% CI, -0.16 to 0.45], $P = 0.33$), which did not. Comparing eyes with and without vitreomacular traction, there were no differences found for inner fluid volume ($0.010 \pm 0.0090 \text{ mm}^3$ vs. $0.019 \pm 0.016 \text{ mm}^3$, respectively; $P = 0.087$), outer fluid volume ($0.078 \pm 0.060 \text{ mm}^3$ vs. $0.012 \pm 0.080 \text{ mm}^3$, respectively; $P = 0.15$), and the total fluid volume ($0.088 \pm 0.064 \text{ mm}^3$ vs. $0.14 \pm 0.083 \text{ mm}^3$, respectively; $P = 0.052$).

Relationship of Postoperative Visual Acuity to Retinal Fluid Volume

Postoperative 12-month visual acuity significantly improved compared with preoperative VA (Mean [SD] VA, 0.12 [0.16] logMAR vs. 0.63 [0.30] logMAR, respectively; $P < 0.0001$). In comparing postoperative 12-month visual acuity to the baseline parameters, univariate analyses showed that inner fluid volume (correlation coefficient = 0.45, [95% CI, 0.15–0.67], $P = 0.0043$) and minimum MH size (Correlation coefficient = 0.45, [95% CI, 0.16–0.67], $P = 0.0036$) were significantly associated with the postoperative 12-month visual acuity, whereas basal MH size, outer fluid volume, and total fluid volume were not (Table 2). A separate analysis of fluid volume inside and outside of 1.5-mm circle centered on the fovea (Supplemental Table 1, Supplemental Digital Content 1, <http://links.lww.com/IAE/B810>) found that inner fluid volume outside the 1.5-mm diameter of the fovea was associated with worse postoperative visual acuity ($P = 0.0017$), whereas inner fluid volume inside the 1.5-mm diameter showed a trend of reduced visual acuity, but this was not statistically significant ($P = 0.057$).

When inner retinal fluid volume was divided into tertiles—small, medium, and large; small inner fluid volume had significantly better visual acuity at one year compared with eyes with large inner fluid volume (Mean [SD] VA, 0.033 [0.094] logMAR [Snellen equivalent, 20/20] vs. 0.20 [0.20] logMAR [Snellen equivalent, 20/32], $P = 0.019$). A similar comparison using tertiles of International Vitreomacular Traction Study–based macular hole sizes found no statistically significant differences among small, medium, and large MH (Table 3).

An exploratory analyses demonstrated that the minimum MH size and total fluid volume were potential confounding factors for the relationship between inner fluid volume and postoperative visual

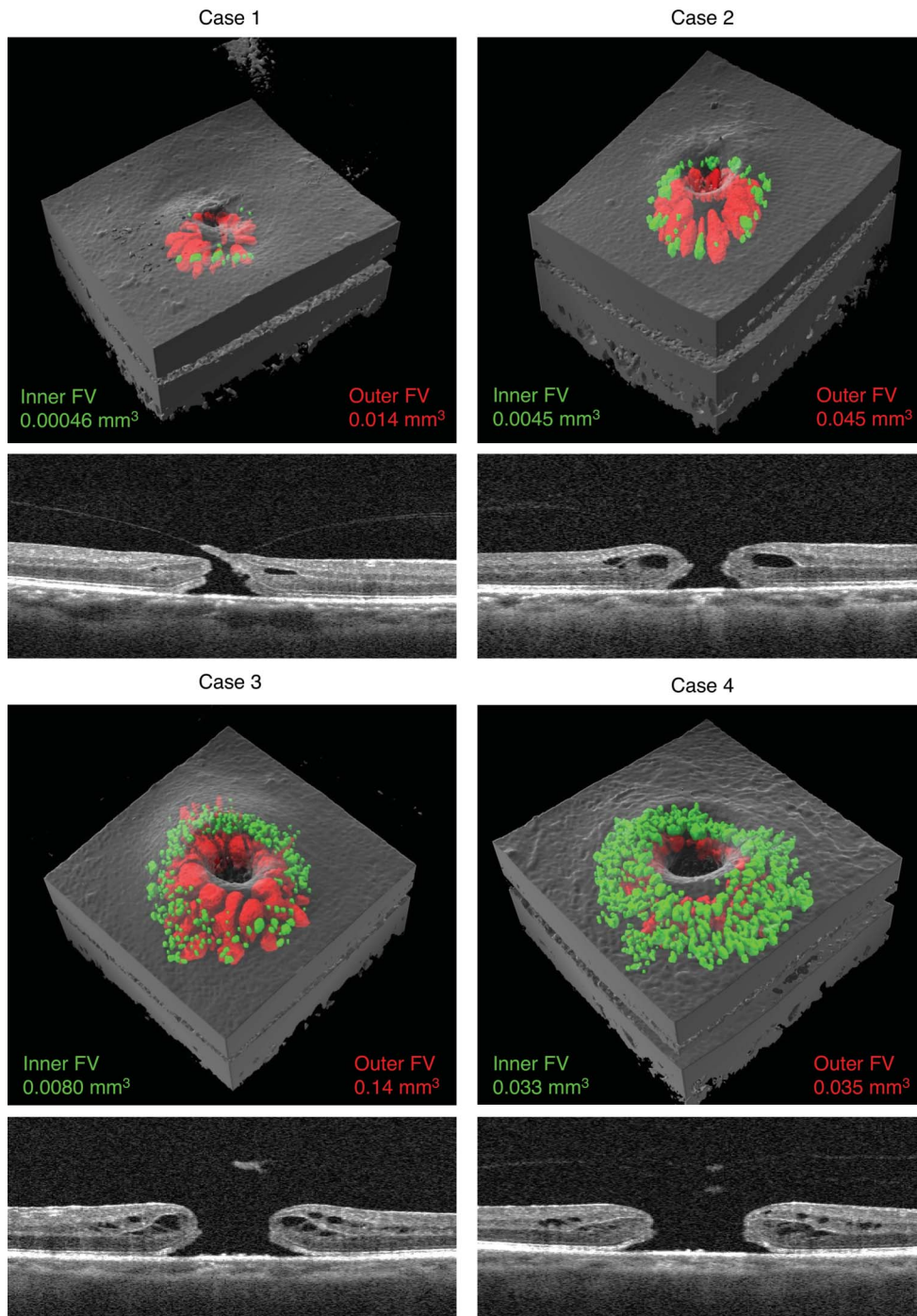


Fig. 2. Volume-rendered OCT illustrates inner fluid (green) and outer fluid (red) in four cases of MH. Case 1: Small MH with VMT with the outer fluid visualized as radial patterns fairly uniformly distributed around the MH, whereas the inner fluid distribution is asymmetrically distributed around the MH. Case 2: Small MH without VMT showing that inner fluid is asymmetrically distributed to outer fluid. Case 3: Large MH without VMT with increased numbers of inner fluid spaces predominantly peripheral and asymmetrically distributed compared with outer fluid. Case 4: Large MH without VMT with densely packed inner fluid spaces distributed evenly around the hole. Minimum MH size of case 3 was similar to that of case 4 (546 μm and 580 μm , respectively), whereas inner fluid volume of case 4 was 4 times larger than that of case 3 (0.0080 mm³ and 0.033 mm³, respectively). Postoperative 12-month visual acuity in case 3 was 0.046 logMAR (almost equal to 20/25), whereas 12-month visual acuity in case 4 was 0.30 logMAR (equal to 20/40).

acuity (changes in correlation coefficient of inner fluid volume: -37% and $+27\%$, respectively), but the basal MH size and outer fluid volume were not. Multivariable analysis revealed that inner fluid volume remained statistically significant for 12-month visual acuity ($P = 0.025$) after accounting for minimum MH size and total fluid volume (Table 2). Before MH surgery, 36 eyes (92%) were phakic, and each

of these eyes underwent successful cataract surgery with lens implantation at the time of MH surgery. Eleven eyes (28%) were graded as two nuclear opacification, and 28 eyes (72%) were graded as three nuclear opacification. There were no differences in the baseline or the postoperative 12-month visual acuity between different cataract grades ($P = 0.33$ and $P = 0.48$, respectively).

fluid volume may be an independent predictor of post-operative visual acuity.

In MH, both mechanical stress¹⁸ and osmotic stress^{19,20} have been proposed to induce the Müller cell dysfunction. Müller cells are essential for controlling homeostasis of fluid and ionic concentrations in the retina.^{21–23} Prior OCT studies demonstrated that intraretinal cystoid spaces start from within the HFL and the ONL during impending MH.^{1,2} The hydration theory proposed by Tornambe²⁴ states that fluid influx into the hole is a critical factor for the progression of full-thickness MH. Once full-thickness MH develops, vitreous fluid gains access to the retina and the increase of fluid influx accelerates the osmotic stress for the Müller cells, resulting in the Müller cell dysfunction. Our quantitative results support these theories. We found that outer fluid seems to increase during early MH formation then stabilizes. In contrast, the inner fluid increased along with the progression to larger MH (Figure 2). Subgroup analysis showed that inner fluid volume increased between two examinations and was correlated with the duration between

Prior studies have shown that certain two-dimensional OCT parameters, such as MH size and height, could predict postoperative visual outcomes.¹⁵ Multiple studies have shown that larger minimum MH size measured with OCT is associated with worse postoperative visual acuity.^{15–17} In this study, the inner fluid volume and minimum MH size were both significantly associated with postoperative VA in the univariate analysis. Because the minimum MH size was a potential confounder for the association between inner fluid volume and postoperative visual acuity, multivariable regression analysis demonstrated that the inner fluid volume remained a statistically significant predictor for postoperative visual acuity. These collective findings provide evidence that the inner

| Baseline Parameters | Univariate Analysis | | | Multivariable Analysis | |
|---|--------------------------|-------------------------------|----------|------------------------------|----------|
| | β (95% CI) | Standardized β (95% CI) | <i>P</i> | β (95% CI) | <i>P</i> |
| Minimum MH size, per 100 μm larger | 0.047 (0.016–0.077) | 0.45 (0.16–0.67) | 0.0036 | 0.029 (–0.0055–0.063) | 0.098 |
| Basal MH size, per 100 μm larger | 0.015 (–0.0068–0.037) | 0.22 (–0.098–0.50) | 0.17 | | |
| Inner FV, per 0.01 mm^3 greater | 0.052 (0.017–0.086) | 0.45 (0.15–0.67) | 0.0043 | 0.047 (0.0063–0.088) | 0.025 |
| Outer FV, per 0.01 mm^3 greater | –0.0042 (–0.011–0.0030) | –0.19 (–0.48–0.13) | 0.25 | | |
| Total FV, per 0.01 mm^3 greater | –0.0021 (–0.0090–0.0049) | –0.099 (–0.40–0.22) | 0.55 | –0.0063 (–0.013–0.000048) | 0.052 |

Copyright © by Ophthalmic Communications Society, Inc. Unauthorized reproduction of this article is prohibited.

Table 3. Comparison in Baseline and 1-Year Postoperative Visual Acuity

| | Inner Fluid Volume* | | | P | | | |
|--|-----------------------------|-------------------------|-------------------------|------------------|----------------------------|------------------------|----------------------------|
| | Small (N = 10) | Medium (N = 11) | Large (N = 18) | Among Groups† | Small Versus Medium‡ | Small Versus Large‡ | Medium Versus Large‡ |
| Baseline VA logMAR (SD) [Snellen VA] | 0.49 (0.20) [20/63] | 0.65 (0.33) [20/100] | 0.69 (0.31) [20/100] | 0.0040 | 0.038 | 0.0039 | 0.64 |
| 1-year logMAR VA (SD) [Snellen VA] | 0.039 (0.083) [20/20] | 0.11 (0.14) [20/25] | 0.16 (0.20) [20/30] | 0.026 | 0.27 | 0.019 | 0.42 |

| | MH size§ | | | P | | | |
|--|-----------------------------|-------------------------|-------------------------|------------------|-------------------------|---------------------------|-------------------------|
| | Small (N = 13) | Medium (N = 13) | Large (N = 13) | Among Groups† | Small Versus Medium‡ | Small Versus Large‡ | Medium Versus Large‡ |
| Baseline logMAR VA (SD) [Snellen VA] | 0.42 (0.17) [20/50] | 0.68 (0.32) [20/100] | 0.78 (0.28) [20/125] | 0.23 | 0.44 | 0.21 | 0.93 |
| 1-year logMAR VA (SD) [Snellen VA] | 0.033 (0.094) [20/20] | 0.11 (0.15) [20/25] | 0.20 (0.20) [20/32] | 0.15 | 0.60 | 0.13 | 0.61 |

*Inner fluid volume was divided into tertiles (Small < 0.00485 mm³, medium between ≥ 0.00485 mm³ and < 0.0194,920,744 mm³, and large ≥ 0.0194,920,744 mm³).

†P value was calculated by analysis of variance.

‡P value was calculated by Tukey–Kramer method.

§MH size was classified based on International Vitreomacular Traction Study classification.

the two examinations, whereas the outer fluid volume was not (Table 4).

Müller cell swelling because of osmotic stress has been shown to result in photoreceptor death and visual impairment.^{19,20} A different study demonstrated that fluid accumulation in the INL had a greater effect on visual acuity and retinal sensitivity than in the OPL in the inflammatory cystoid macular edema.²⁵ These studies support our findings that increased inner fluid volume is associated with worsening postoperative visual acuity. Functional studies have demonstrated that photoreceptors adjacent to the MH are impaired, and these regions do not completely recover after successful MH closure.^{26,27} To assess the impact and distribution of intraretinal fluid on retinal function in MH,

further investigation using examinations for focal retinal function, such as microperimetry or focal macular electroretinograms, would be helpful.

There are several limitations to this study, including a small sample size and retrospective study design. Minimum MH size has been reported to be a common predictor for post-MH surgery visual outcome.^{15–17} However, the current multivariable analysis demonstrated that minimum MH size was not statistically significant for 1-year visual acuity outcome, and there were no differences in baseline visual acuity and 1-year visual acuity among different MH sizes. This unexpected finding could be attributed to the relatively small sample size. The P value of minimum MH size in the multivariable analysis was fairly small (P = 0.098); this might suggest a trend toward significance that

Table 4. Changes in Macular Hole Size and Fluid Volume Between Two Scans

| Parameters (N=20) | Comparisons Between Two Time Point | | | Relationships Between Changes and Duration Between Two Time Points | |
|---------------------------------------|------------------------------------|---------------|--------|--|--------|
| | 1st Visit | 2nd Visit | P | Correlation Coefficient (95% CI) | P* |
| Minimum MH size, μm , (SD) | 325 (125) | 355 (159) | 0.063† | 0.25 (−0.20–0.65) | 0.28 |
| Basal MH size, μm , (SD) | 765 (203) | 792 (204) | 0.097† | 0.25 (−0.23–0.63) | 0.25 |
| Inner FV, mm ³ , (SD) | 0.0089 (0.0091) | 0.013 (0.012) | 0.016‡ | 0.76 (0.27–0.90) | 0.0002 |
| Outer FV, mm ³ , (SD) | 0.090 (0.054) | 0.098 (0.070) | 0.32† | 0.23 (−0.25–0.62) | 0.34 |
| Total FV, mm ³ , (SD) | 0.099 (0.057) | 0.11 (0.074) | 0.20† | 0.34 (−0.14–0.69) | 0.16 |

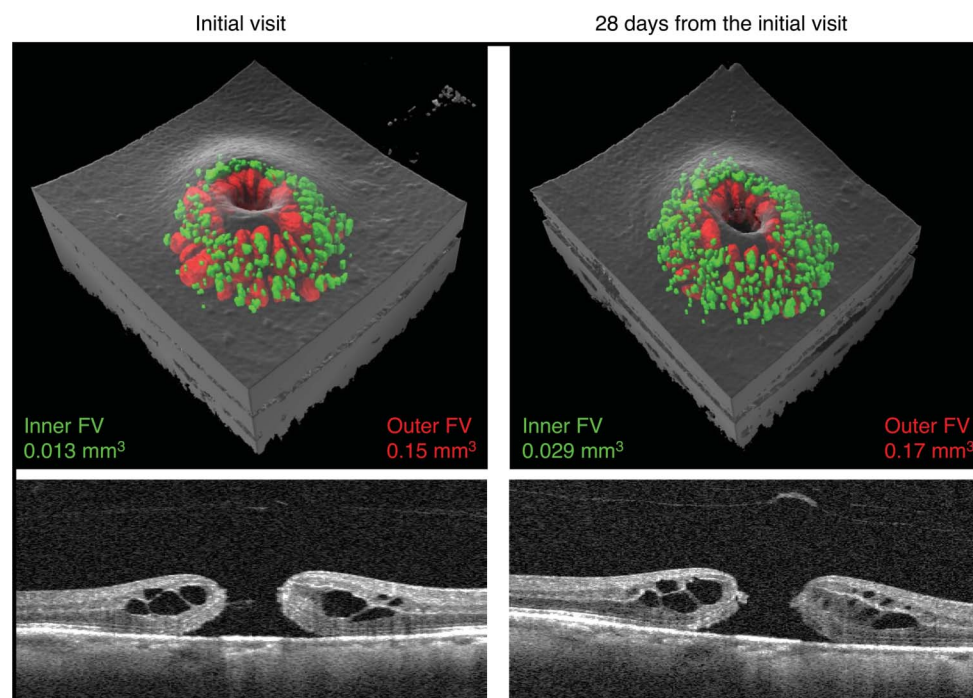
FV, fluid volume.

*Pearson correlation coefficient.

†Paired t test.

‡Wilcoxon-signed rank test.

Fig. 3. The changes in fluid volume between the two scans. At the initial visit, the outer fluid volume (red) and inner fluid volume (green) surround the macular hole. After 28 days, the inner fluid volume increased more than two-fold compared with only a 10% increase in outer fluid volume.



may be achieved in a future study with a larger sample size. Because of the small sample size, larger studies are needed to validate our findings that inner fluid volume is associated with postsurgical visual acuity. This study included three pseudophakic patients before the MH surgery; however, we did not perform FA to exclude Irvine–Gass syndrome, and it is unknown if the presence of prior Irvine–Gass syndrome could affect the intraretinal fluid accumulation. This seems less likely because in each case, the cataract surgery at least 12 months before the baseline examination. Our results are limited to macular holes with less than 1 year of duration, and it is unknown how useful a biomarker of inner fluid volume would be in eyes with chronic macular holes when intraretinal cystoid spaces are less frequently found.²⁸ Similar to the loss of intraretinal cystoid spaces over time associated with worsening geographic atrophy in age-related macular degeneration, loss of intraretinal cystoid spaces in more chronic macular holes likely indicates greater tissue atrophy and degeneration.²⁹ Eyes included in this study had different surgical procedures, such as 25-gauge and 27-gauge system, different types of gas tamponade, and a Brilliant Blue contrast dye was used.³⁰ It is unknown if these surgical techniques could have affected visual acuity and we have not accounted for it. Finally, three-dimensional OCT-based fluid volume assessment is not available in the current clinical setting. However, with the advancement of OCT imaging and deep learning-based algorithms,^{9,10} three-dimensional assessment of fluid volume will likely soon be available in the clinic setting.

In conclusion, this pilot study demonstrated that three-dimensional quantification revealed that increased inner fluid volume is associated with greater MH size and decreased postoperative visual acuity after successful MH surgery. Inner fluid volume spatial localization peripheral to macular hole is consistent with Z-shaped Müller cell configuration. By contrast, outer fluid volume remained stable with MH progression and was not associated with postoperative visual acuity. These findings suggest that the inner fluid volume is associated with more advanced MH and is sign of Müller cells dysfunction and possibly evidence of retinal degeneration.

Key words: full-thickness macular hole, MH, fluid volume, volume-rendering OCT, Muller cell, visual prognosis.

Acknowledgments

The authors thank Ms. Yumi Fujita, a research assistant, for her work managing, collecting, and inputting the clinical data, and Dr. Yuichiro Ishida for collecting the data.

References

1. Kishi S, Kamei Y, Shimizu K. Tractional elevation of Henle's fiber layer in idiopathic macular holes. *Am J Ophthalmol* 1995; 120:486–496.
2. Gaudric GA, Haouchine B, Massin P, et al. Macular hole formation: new data provided by optical coherence tomography. *Arch Ophthalmol* 1999;117:744–751.

3. Matet A, Savastano MC, Rispoli M, et al. En face optical coherence tomography of foveal microstructure in full-thickness macular hole: a model to study perifoveal Müller cells. *Am J Ophthalmol* 2015;159:1142–1151.
4. Chung H, Byeon SH. New insights into the pathoanatomy of macular holes based on features of optical coherence tomography. *Surv Ophthalmol* 2017;62:506–521.
5. Govetto A, Sarraf D, Hubschman J-P, et al. Distinctive mechanisms and patterns of exudative versus tractional intraretinal cystoid spaces as seen with multimodal imaging. *Am J Ophthalmol* 2020;212:43–56.
6. Goto K, Iwase T, Yamamoto K, et al. Correlations between intraretinal cystoid cavities and pre- and postoperative characteristics of eyes after closure of idiopathic macular hole. *Sci Rep* 2020;10:2310.
7. Gass JD. Reappraisal of biomicroscopic classification of stages of development of a macular hole. *Am J Ophthalmol* 1995;119:752–759.
8. Bringmann A, Reichenbach A, Wiedemann P. Pathomechanisms of cystoid macular edema. *Ophthalmic Res* 2004;36:241–249.
9. Guo Y, Hormel TT, Xiong H, et al. Automated segmentation of retinal fluid volumes from structural and angiographic optical coherence tomography using deep learning. *Transl Vis Sci Technol* 2020;9:54.
10. Schmidt-Erfurth U, Vogl W-D, Jampol LM, et al. Application of automated quantification of fluid volumes to anti-VEGF therapy of neovascular age-related macular degeneration. *Ophthalmology* 2020;127:1211–1219.
11. Wang J, Zhang M, Pechauer AD, et al. Automated volumetric segmentation of retinal fluid on optical coherence tomography. *Biomed Opt Express* 2016;7:1577–1589.
12. Guo Y, Camino A, Zhang M, et al. Automated segmentation of retinal layer boundaries and capillary plexuses in wide-field optical coherence tomographic angiography. *Biomed Opt Express* 2018;9:4429–4442.
13. Duker JS, Kaiser PK, Binder S, et al. The International Vitreomacular Traction Study Group classification of vitreomacular adhesion, traction, and macular hole. *Ophthalmology* 2013;120:2611–2619.
14. Bennett AG, Rudnicka AR, Edgar DF. Improvements on Littmann's method of determining the size of retinal features by fundus photography. *Graefes Arch Clin Exp Ophthalmol* 1994;32:361–367.
15. Ip MS, Baker BJ, Duker JS, et al. Anatomical outcomes of surgery for idiopathic macular hole as determined by optical coherence tomography. *Arch Ophthalmol* 2002;120:29–35.
16. Ullrich S, Haritoglou C, Gass C, et al. Macular hole size as a prognostic factor in macular hole surgery. *Br J Ophthalmol* 2002;86:390–393.
17. Mehta N, Lavinsky F, Laroche R, et al. Assessing the ability of preoperative quantitative spectral-domain optical coherence tomography characteristics to predict visual outcome in idiopathic macular hole surgery. *Retina* 2021;41:29–36.
18. Lindqvist N, Liu Q, Zajadacz J, et al. Retinal glial (Müller) cells: sensing and responding to tissue stretch. *Invest Ophthalmol Vis Sci* 2010;51:1683–1690.
19. Francke M, Faude F, Pannicke T, et al. Glial cell-mediated spread of retinal degeneration during detachment: a hypothesis based upon studies in rabbits. *Vis Res* 2005;45:2256–2267.
20. Matsumoto H, Sugio S, Seghers F, et al. Retinal detachment-induced Müller glial cell swelling activates TRPV4 ion channels and triggers photoreceptor death at body temperature. *J Neurosci* 2018;38:8745–8758.
21. Bringmann A, Pannicke T, Grosche J, et al. Müller cells in the healthy and diseased retina. *Prog Retin Eye Res* 2006;25:397–424.
22. Daruich A, Matet A, Moulin A, et al. Mechanisms of macular edema: beyond the surface. *Prog Retin Eye Res* 2018;63:20–68.
23. Spaide RF. Retinal vascular cystoid macular edema: review and new theory. *Retina* 2016;36:1823–1842.
24. Tornambe PE. Macular hole genesis: the hydration theory. *Retina* 2003;23:421–424.
25. Munk MR, Kiss CG, Huf W, et al. Visual acuity and microperimetric mapping of lesion area in eyes with inflammatory cystoid macular oedema. *Acta Ophthalmol* 2014;92:332–338.
26. Terasaki H, Miyake Y, Tanikawa A, et al. Focal macular electroretinograms before and after successful macular hole surgery. *Am J Ophthalmol* 1998;125:204–213.
27. Amari F, Ohta K, Kojima H, et al. Predicting visual outcome after macular hole surgery using scanning laser ophthalmoscope microperimetry. *Br J Ophthalmol* 2001;85:96–98.
28. Yun C, Oh J, Hwang SY, et al. Morphologic characteristics of chronic macular hole on optical coherence tomography. *Retina* 2012;32:2077–2084.
29. Pasricha MV, Tai V, Sleiman K, et al. Local anatomic precursors to new-onset geographic atrophy in age-related macular degeneration as defined on OCT. *Ophthalmol Retina* 2021;5:396–408.
30. Essex RW, Hunyor AP, Moreno-Betancur M, et al. The visual outcomes of macular hole surgery: a Registry-Based Study by the Australian and New Zealand Society of retinal specialists. *Ophthalmol Retina* 2018;2:1143–1151.